HAIT Journal of Science and Engineering B, Volume 2, Issues 3-4, pp. 529-557

Application of duality for derivation of current converter topologies

Doron Shmilovitz

Faculty of Engineering, Tel-Aviv University,
Tel-Aviv 69978, Israel
e-mail: shmilo@eng.tau.ac.il

Received 1 April 2005, accepted 20 July 2005

Abstract

A unified approach is suggested for the derivation of current-to-current converter topologies, which relies on duality principles. As conventional duality rules have restricted utility and are difficult to apply with switched mode circuits, special attention is devoted to switch mode converter element dualities. Also, a special means of viewing complex switched mode topologies as a cascade combination of building blocks is developed. This method simplifies the treatment of circuits containing transformers and switching bridges.

The suggested approach provides a universal means for derivation of current-to-current converters by dually transforming voltage-to-voltage converter topologies.

Examples of the utilization of this method for derivation of various current-to-current converters, including Buck, Boost, Buck-Boost, Čuk, Sepic, and Two-Switch Forward, are provided, as well as a practical design example for SMES (Superconducting Magnetic Energy Storage) application.

Keywords: Duality, current converter, current source, switched mode power converters.

1 Introduction

To a large extent, DC-DC converters may be regarded as DC transformers, this is due to their high efficiency which implies energy conservation, as well as due to their output voltage being proportional to their input voltage and vice versa: the input current of a DC-DC converter is proportional to the output current [1]. This approach is most attractive due to a special feature of this particular family of transformers: the so called 'controllable transfer ratio'. This feature provides the most important means for the improvement of the system's performance (through the application of various control schemes to tune continuously the converter's transfer ratio). However, unlike the ideal transformers mathematical model (which allow for the connection of any type of source at its input as long as it complies with the load characteristics at the output), converter realized transformer behavior is realization dependent. Namely, the types of source and loads suitable for connection at the converter's terminals depend upon the converter implementation. Since the majority of power sources are actually voltage sources, most converter topologies have evolved under the assumption that the converter input should accommodate a voltage source at its input (this is the reason that most of the converters are based on a switched inductor cell [1]). This, in addition to the transformer-like behavior of these converters, yields voltage source characteristics at the converter output as well. Thus application of a rather stiff current type of source is not possible for most of the converters. However, current source types of power sources do exist [1-5]. They include large inductors initially charged to high currents such as superconducting coils in Superconducting Magnetic Energy Storage (SMES) systems. These systems are applied to either provide power during short voltage sags or for the generation of high magnetic fields [2], see Fig. 1.

Large utility (or generators) source impedances (which are, to a large extent, of inductive nature) feeding a switched mode converter would also exhibit current source characteristics at the converter's input. Additionally, the DC input to switched-mode converters is often obtained by rectification and filtration the AC mains. To reduce current harmonics and EMI noise, the rectifier most often includes a large filter inductor (choke), at either side of the rectifying bridge, which might eventually introduce a current source like behavior at the rectifier output – the switched mode converter's input [5].

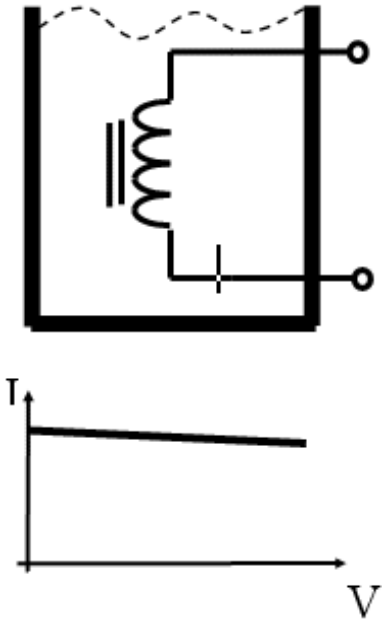

Figure 1: A superconductive magnetic energy storage coil and its current source like I-V characteristics.

In current fed converters a constant current is established through an inductor, whose continuity is ensured by the overlapped on-states of the switches that direct this current. In this kind of circuit, the current source is practically established at an inner point of the circuit and the sub-circuit from this point on may be regarded as a current converter. A similar situation occurs in some resonant converter topologies [1,7,8].

Other power sources exhibit current source behavior when operated in a certain region of their I-V curve, for instance, a photovoltaic generator, as depicted in Fig. 2.

This type of source is sometimes regarded as a current source, which, for instance, affects the power system topology of solar array powered earth-orbiting spacecrafts. In these systems the DC bus voltage is regulated by dissipative shunt elements and the solar panels outputs are added together in a parallel connection [1,4,9]. At the converter's output, some loads may be better and rather stable operated while energized by a current source rather than voltage sources. Such characteristics are required when ener-

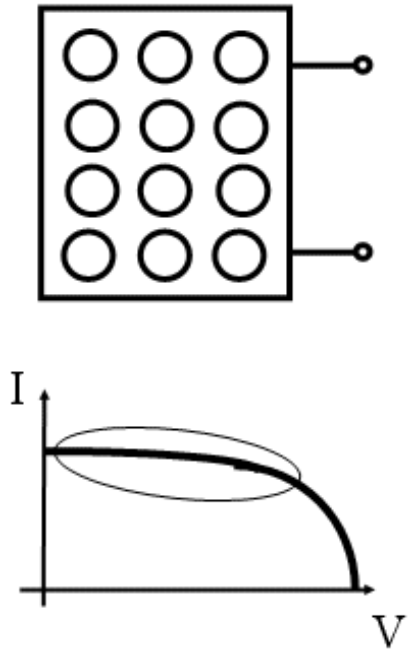

Figure 2: A solar panel and its current source like region of operation.

gizing loads with constant voltage like spark gaps and electric arcs. So are gas discharge devices (like gas lasers) that exhibit negative impedance at certain operation points. Application of voltage type sources to such loads might cause instable oscillations (such applications are reported in [10,11], where transmission line segments have been employed to form a high frequency electronic ballast for HID lamps). It has been attempted to address this problem by application of current mode control, which provides a fair solution in some cases [12]. Yet a converter topology that exhibits inherent current source characteristics at its output (the kind that results from the power stage topology rather than control implied) should offer much more stability and robustness. Indeed, a few attempts at the development of current-to-current converter topologies have been reported, which incorporate duality principle [2,3,5,9,13-16]. The theory of duality is known to be an important and a widely used one for analysis, as well as synthesis, within the field of electrical networks since long ago [17,18]. Later on, duality has

been employed in the field of switched mode converters for analysis purpose. This promoted the understanding of switched mode converter circuits and the relations between different converter topologies [19,20]. The potential of duality as a tool for the development of power converters topologies was realized later on. Major contributions to duality in the context of power electronics topologies were made by Freeland [21,22] and by Wolfs *et al.* [14-16]. The former developed novel dual models for power converter building blocks such as semiconductor switches, switching bridges, and practical inductors and transformers [21,22]. In the second group of publications, [16], duality has been extensively employed for the derivation of a current-sourced link converter [14,15]. The possible application of duality to nonplanar topologies has been facilitated as well [16].

In this work, a systematic approach is suggested for derivation of current-to-current converter topologies from known voltage-to-voltage converter topologies, employing a simple and consistent set of rules arising from duality principle. As voltage-to-voltage converters have been around for over three decades, a large variety of such topologies already exist. Therefore the approach suggested herein, of deriving current-to-current converter topologies from existing voltage-to-voltage converter topologies, seems reasonable. An alternative procedure to the previously proposed π-T dual transformation [5,22] based on graph transformation is proposed. This procedure might be simpler to employ for some of the power conversion topologies. Another simplification is offered by viewing a given circuit as a cascade combination of few two-port-subcircuits. In most of the cases, the dual transformation may be reached by application of duality to each of the two-port-subcircuits, then reconnecting them in a cascade. In such a manner, the dualities of circuits including complex structures, such as switching bridges, can be rather easily derived.

2 Duality principle

Some of the basic duality rules (applications of duality to linear components) are reviewed herein. Then, an application method of duality to nonlinear components and to complex graphs, which are of interest for converter synthesis, is derived. Distinction is made between graph transformation and network elements transformation (components transformation).

2.1 Network elements (components) transformation

Passive components duals are obtained through their reciprocal impedances:

$$Z = Y^D \quad \Rightarrow \quad Z^D(j\omega) = (Z(j\omega))^{-1} \tag{1}$$

where Z and Y represent impedance and admittance, respectively, and the superscript '^{D}' stands for 'dual'. Equation (1) implies that inductors map into capacitors of equal numerical value:

$$L^D = C \;\; ; \;\; C = 1\tfrac{F}{Hy} \cdot L \;\; . \tag{2}$$

Capacitors map into inductors of equal value:

$$C^D = L \;\; ; \;\; L = 1\tfrac{Hy}{F} \cdot C \;\; . \tag{3}$$

Ideal transformers map into transformers with inverse transfer ratio:

$$1 : k \quad \longrightarrow \quad k : 1 \;\; . \tag{4}$$

Transformers are therefore invariant to dual transformation (in terms of component nature rather than value, similarly to pure resistances and unlike reactive components). It should be noted that practical transformers inherently contain stray inductances (leakage inductances in series with the primary and secondary windings and magnetizing inductances in parallel with them). These inductances will remain in the dual transformer and might cause high voltages if currents are forced through them. This difficulty regarding transformer dualities has been observed and comprehensively analyzed in [22] (as well as the nonlinear phenomena of magnetic saturation). Transformers that are based upon capacitive coupling, such as piezoelectric transformers, might enable a better realization of transformer duals.

Voltage source duals are current sources of equal value and vice versa; current source duals are voltage sources of equal value.

$$(V_S)^D = I_S; \quad I_S = 1\tfrac{Amp}{Volt} \cdot V_S \;\; , \tag{5}$$

$$(I_S)^D = V_S; \quad V_S = 1\tfrac{Volt}{Amp} \cdot I_S \;\; . \tag{6}$$

Switches and switching bridges are frequently employed building blocks of power converters. Therefore they deserve special attention. Equation (1) indicates that the reciprocal of zero impedance is an infinite impedance (open circuit) and that of an open circuit is a '0' impedance (short circuit).

Therefore, a closed switch maps into an open one and vice versa, an open switch maps into a closed one (see Fig. 3):

$$x^D = \bar{x}. \tag{7}$$

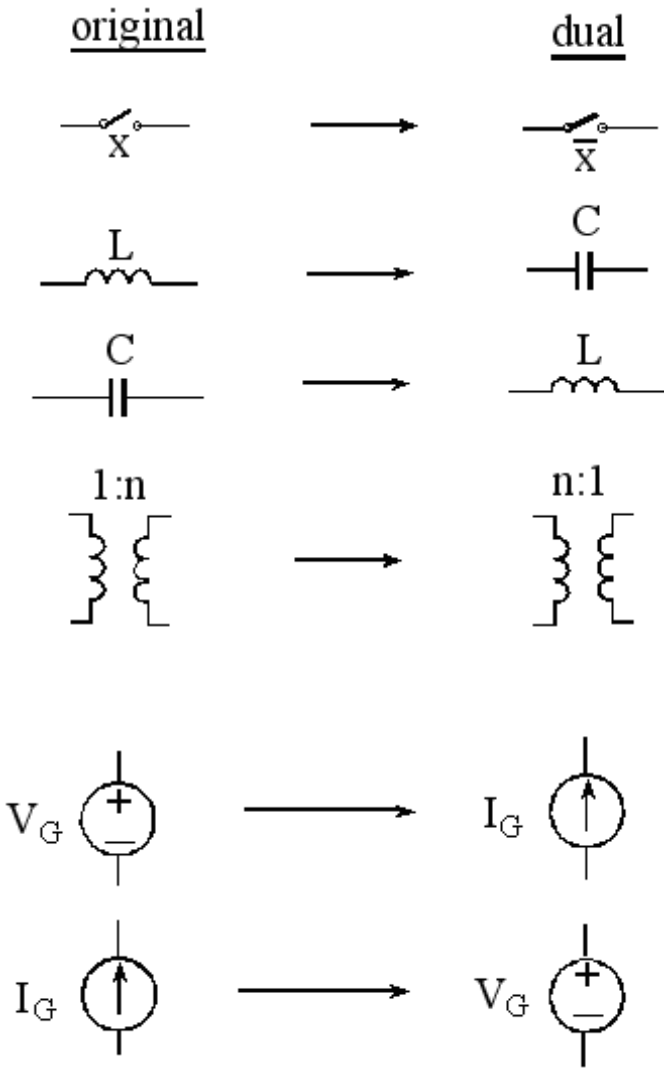

Figure 3: Main components of switched mode converters and their duals.

2.2 Graph transformation

The primitive (original) network should be described as a graph combination of branches. A dual graph may then be derived by transforming every couple of branches connected in parallel into a series connection of the dual branches and vice versa: transforming every couple branches connected in series into a parallel connection of the dual branches. This process must be carried out successively, until the entire graph is represented by basic branches (branches that consist of no more sub-branches). For instance, the graph in Fig. 4a transforms into that of Fig. 4b where **a**, **b**, **c** and **d** represent three branches in the original network and $\mathbf{a}^D$, $\mathbf{b}^D$, $\mathbf{c}^D$ and $\mathbf{d}^D$ represent their duals, respectively.

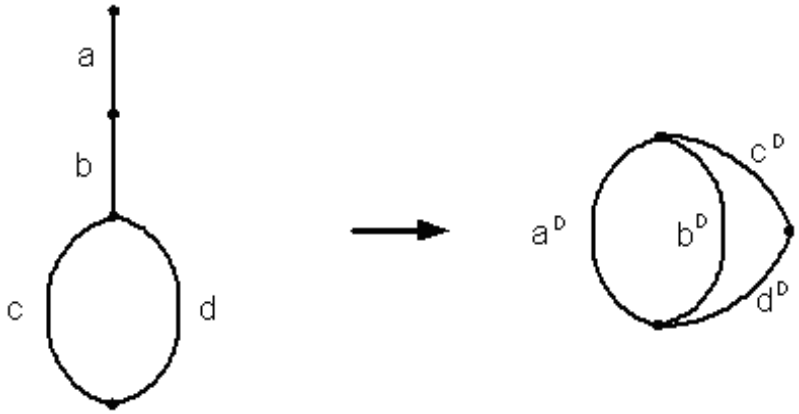

Figure 4: Dual graph transformation.

Two-port elements (TPE), such as transformers and switching bridges call for special treatment. Whenever possible, a network that contains such a TPE (two-port-element) should be divided into two separate sub-networks coupled by the two-port element, see Fig. 5a. By duality, this network is, than transformed into that of Fig. 5b. If the TPE is a transformer, its dual is a transformer as well, as indicated by (4).

Consider a switching bridge, implemented by two single-pole-dual-throw switches as shown in Fig. 6.

For a planar circuit it is possible to find its dual by graph transformation [22] or by oriented graph as discussed in [18]. An alternative, easy to apply method is suggested: while the switches are in position 1, the bridge input voltage (V_G, in this case) is applied to the bridge output, whereas while the

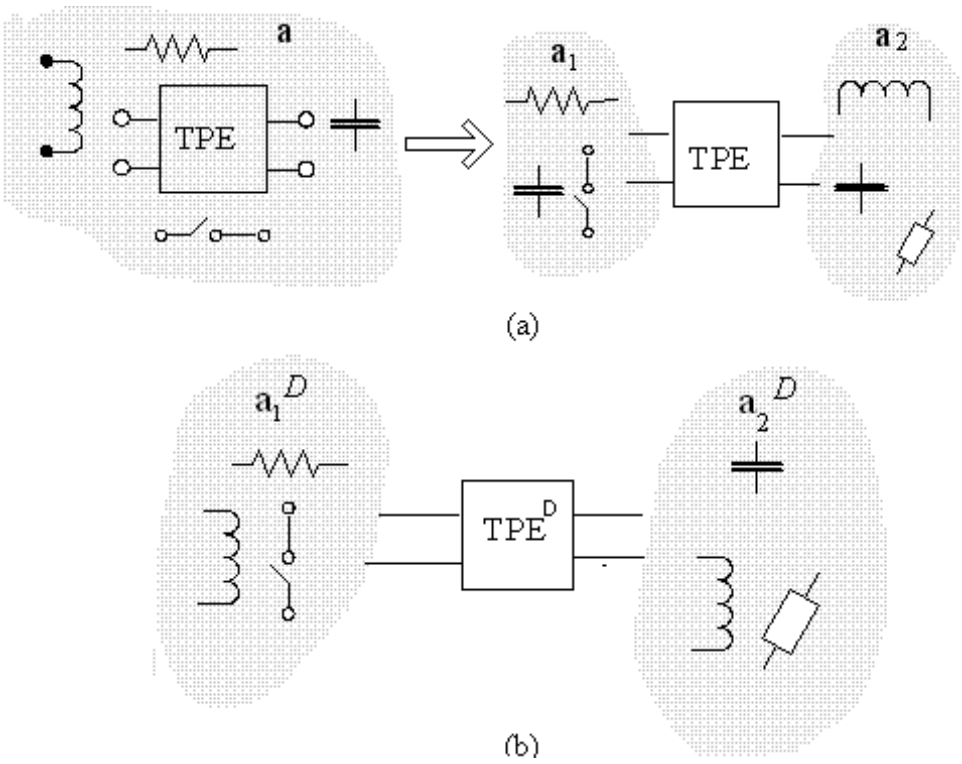

Figure 5: Two port elements coupling two subcircuits (a), and its dual transformation (b).

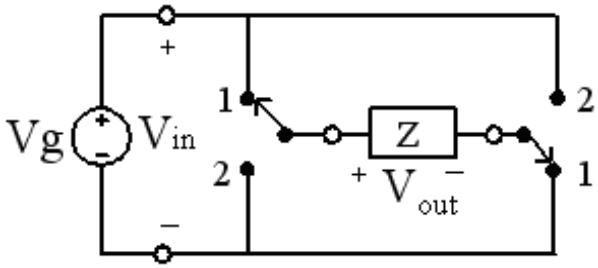

Figure 6: A switching bridge.

switches are in position 2, the polarity is reversed. Therefore, its action is equivalent to that of a virtual transformer with a controllable turns-ratio $k(t)$

$$k(t) = \begin{cases} 1 & s = 1 \\ -1 & s = 2 \end{cases} \tag{8}$$

as depicted in Fig. 7.

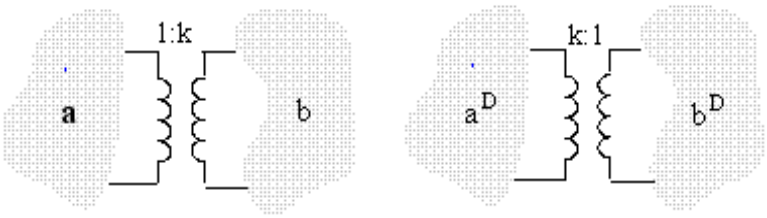

Figure 7: The virtual variable transformer model of the switching bridge and its dual.

Since k is either 1 or (-1), the virtual transformer maps into a virtual transformer with the same instantaneous turns ratio (4). This inverting switching bridge is thus invariant to dual transformation. To ensure practical operation, duality should be applied not only to circuit elements but also to switching functions. If, for instance, **a** in Fig. 7 is a voltage source, a dead time must be implemented in the switching bridge in order to prevent shoot-through currents. Whereas, in the dual circuit (Fig. 7b), $\mathbf{a}^D$ is a current source, and an overlapping of the on states will automatically result by application of duality to the switching function, ensuring current continuity.

Switching bridges are often employed in power converters in conjunction with a transformer to form an alternating signal at the transformers input. This is actually a cascade connection of two two-port-elements (Fig. 8). Applying the duality rule for cascade connection successively (for each TPE) would result in a similar cascade topology in which each of the networks in each of the two two-port-elements is replaced by its dual element, see Fig. 8.

That is correct in principle, however, details of implementation like those mentioned above must be considered. Similarly, switching bridges that generate zero levels in addition to their input or inversed input, can be treated by analyzing their functionality rather than by the straightforward application of duality. For instance, a three level voltage source inverter generates at the bridge output a waveform as shown in Fig. 9 where $x = \bar{z}$ and $y = \bar{w}$ in order to prevent a short across V_G.

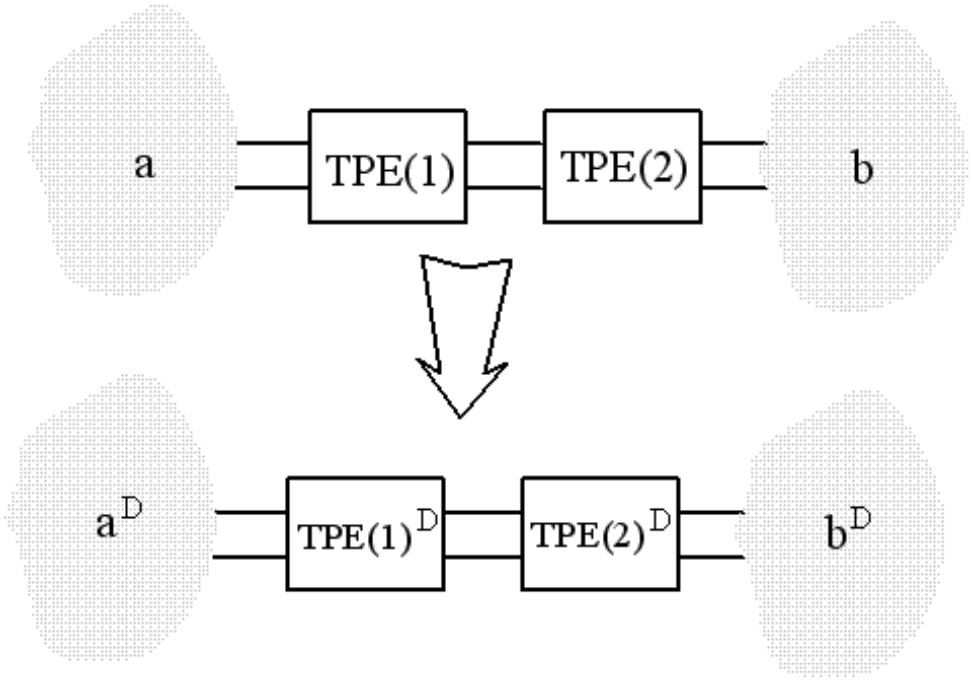

Figure 8: A cascade connection of two two-port-elements and its dual.

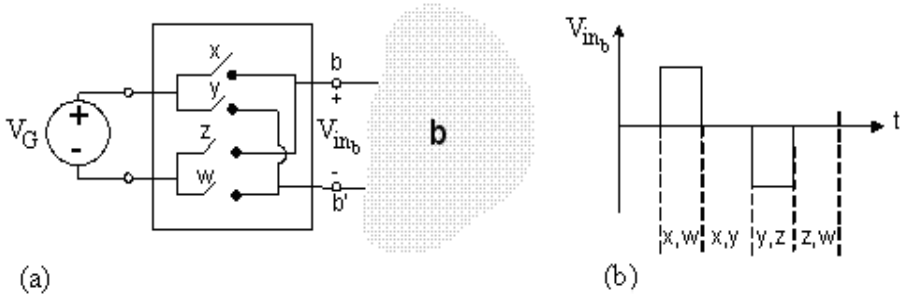

Figure 9: A three level inverter (a) and its output voltage waveform (b).

The varying turns ratio transformer approach cannot be employed in this case since it would involve a turns ratio of either '0' or '∞'. In the dual circuit, a current source should appear at the **b-b'** terminals which has the precisely same waveform as the voltage in the original circuit (Fig. 9b). This

would be accomplished by replacing the voltage source V_G with a current source I_G and exercising the bridge switches differently, as shown in Fig. 10.

The new sequence would be: $x, w \rightarrow x, z \rightarrow y, z$ and y, w. In this dual circuit $x = \bar{y}$ and $z = \bar{w}$ in order to ensure always a closed path for I_G. This approach can serve for the development of various topologies involving switching bridges, such as current source inverters or unity power factor rectifiers, which practically implement a sinusoidal current source with respect to the AC mains.

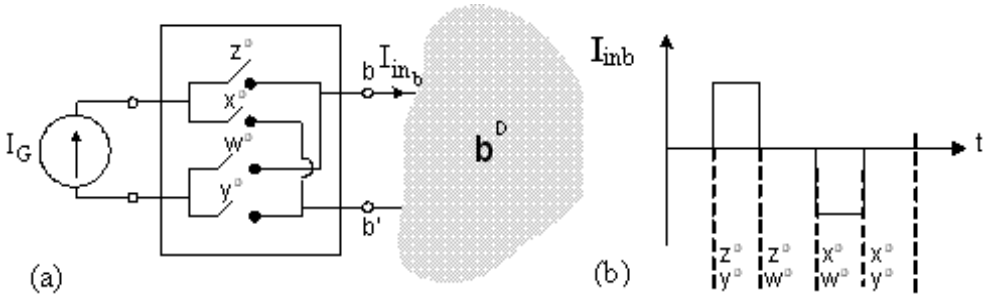

Figure 10: The three level inverter (a) and its output current waveform (b).

3 Derivation of some current-to-current converter topologies

Development of current-to-current converter topologies can be either done from scratch or accomplished by applying some symmetry principles such as horizontally flipping of portions of a voltage converter [4] or by manipulation of a switched capacitor cell [5]. While doing so, some basic requirements must be ensured:

- the converter topology must always provide a current path for the input current source, regardless of the switches states;
- no inductor may connect to the input;
- output parameters (current or voltage) should be controllable via a switching parameter such as the duty ratio, D.

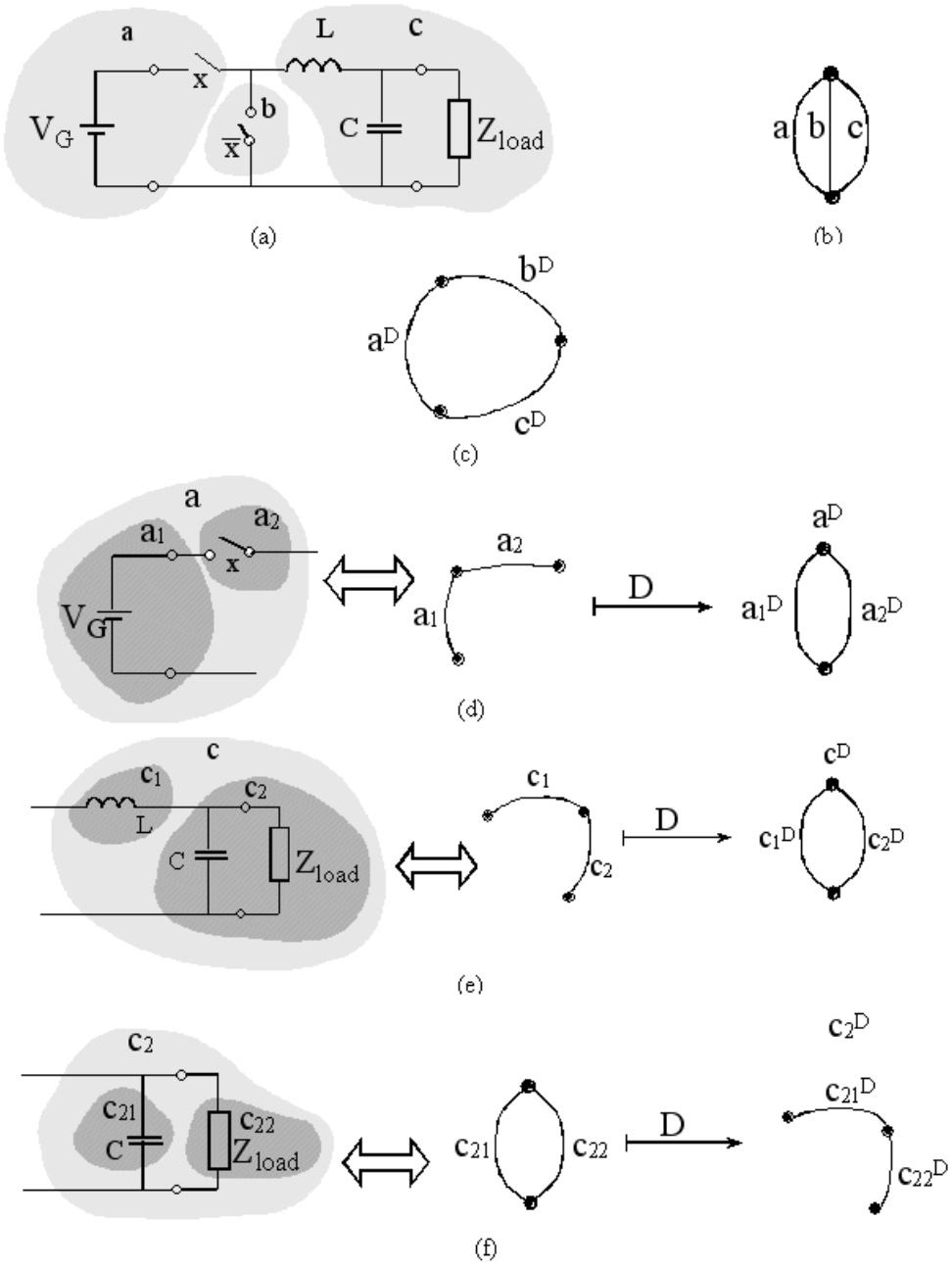

Figure 11: Successive application of the method for a buck topology.

Additionally, the system must be stable under dynamical conditions. When deriving a current-to-current converter topology via the duality method proposed herein, the above mentioned requirements are automatically fulfilled, without special care. Moreover, the same DC voltage gain that applied for the original converter V_O/V_G should be valid for the DC current gain I_O/I_G of the dual converter. Applying the duality rules stated in the previous paragraph, yields some current-to-current converter topologies. Herein are some examples. Consider the voltage buck converter represented by three branches, **a**, **b**, and **c**, as in Figs. 11a and 11b. The original circuits graph is depicted in Fig. 11b. Since these branches are connected in parallel, the graph maps into its dual as shown in Fig. 11c. Branch **a** consists of two branches $\mathbf{a}_1$and $\mathbf{a}_2$ connected in series, which maps therefore as a parallel connection of the dual branches $\mathbf{a}_1^D$and $\mathbf{a}_2^D$ (Fig. 11d). Similarly, branch **c** consists of two branches $\mathbf{c}_1$ and $\mathbf{c}_2$ connected in series, which map into a parallel connection of their duals $\mathbf{c}_1^D$ and $\mathbf{c}_2^D$, as shown in Fig. 11e. $\mathbf{c}_2$ itself consists of two branches $\mathbf{c}_{21}$ and $\mathbf{c}_{22}$ which maps into $\mathbf{c}_2^D$ according to the same rules (Fig. 11f).

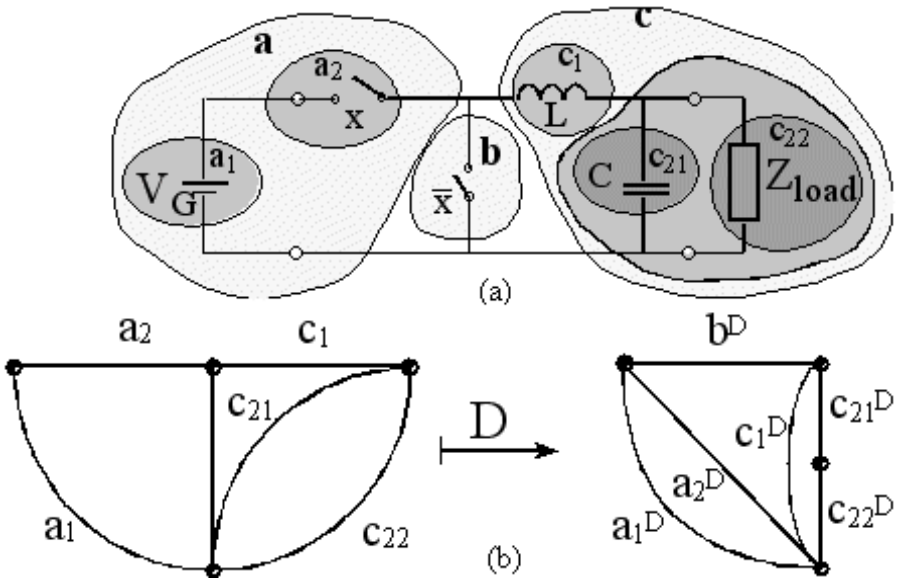

Figure 12: Graph transformation of the buck topology: (a) original circuit; (b) dual transformation.

The graph of the original buck topology can now be represented in terms of basic branches by substitution of each subgraph in the place of the equivalent graph, as shown in Fig. 12a. Performing the same substitution process for the dual sub graphs results in the total dual graph as depicted in Fig. 12b.

In this last graph, each branch is composed of a single network element, which means that each branch can be replaced by the dual network element according to the network elements transformations shown in Fig. 3, resulting in the dual converter topology depicted in Fig. 13.

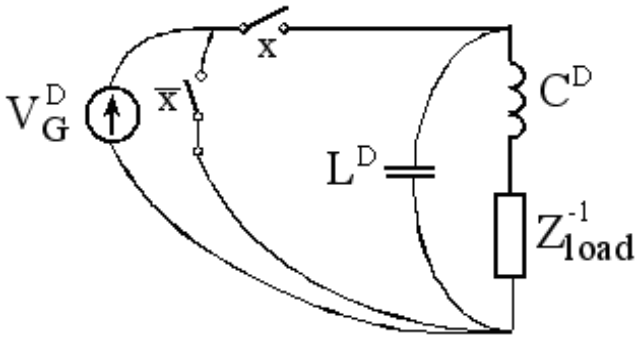

Figure 13: The resulting dual buck topology.

Regardless of component values, the current-to-current topology has been derived, as shown in Fig. 14. It will be shown that it has the DC gain of a buck topology with respect to output to input current ratio.

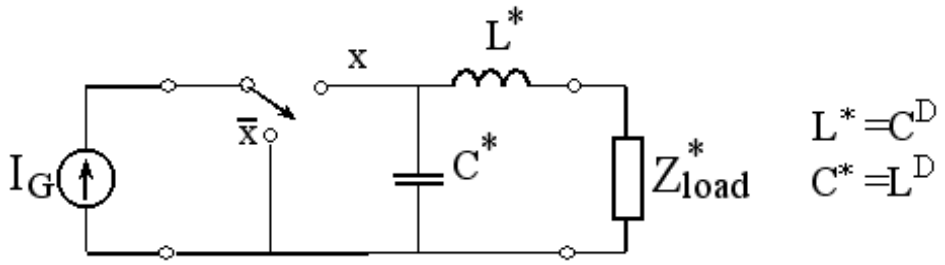

Figure 14: Buck current to current converter.

Similarly, the conventional boost voltage-to-voltage topology and its graph description are shown in Fig. 15. The dual of this graph is derived

via the duality graph transformation rules (Fig. 16a), and finally replacement of each branch by the suitable dual component results in the boost current-to-current converter topology depicted in Fig. 16b.

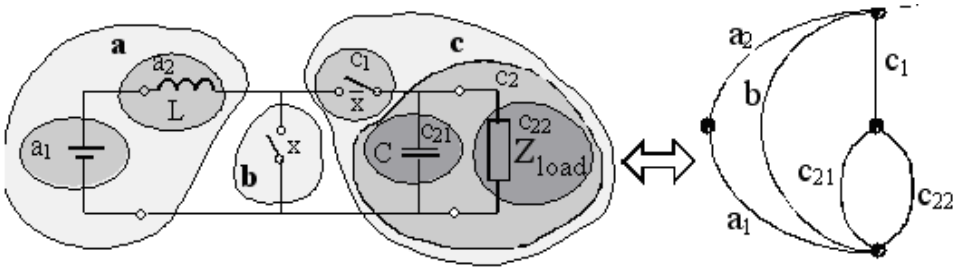

Figure 15: A voltage boost topology (a) and its graph representation (b).

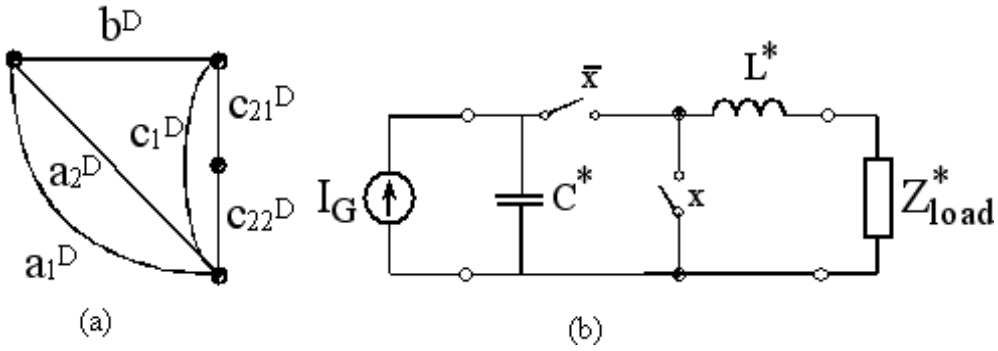

Figure 16: Dual boost derivation: (a) graph transformation; (b) component placement.

A buck-boost voltage-to-voltage topology and its branch assignment are shown in Fig. 17. It may be observed by inspection that this topology is described by the same graph as the boost converter (Fig. 15b), thus the resulting dual graph is also the same (Fig. 16a).

Finally, the buck-boost current-to-current converter topology is obtained by placing the suitable component duals, see Fig. 18 (it may be noted that the only difference with respect to the boost topology arises from substitution of components for branches $\mathbf{a}_2$ and $\mathbf{b}$).

Higher order current-to-current converter topologies can be derived through the same method as well. For instance, when continuous waveforms are desired at the source terminal as well as at the load terminal, a

boost-buck (Čuk) voltage-to-voltage converter might be chosen (Fig. 19).

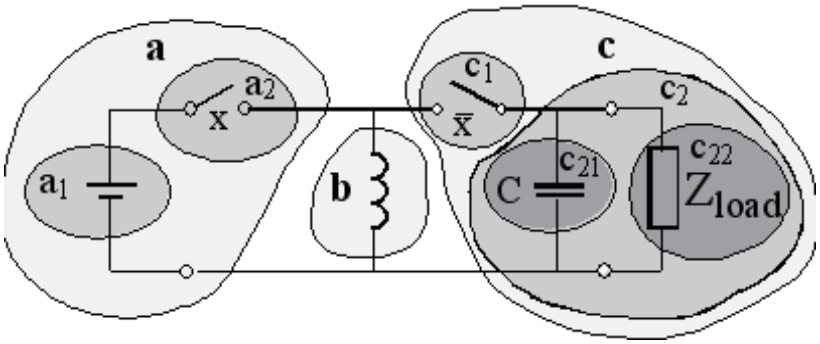

Figure 17: A voltage buck-boost topology and its branch assignment.

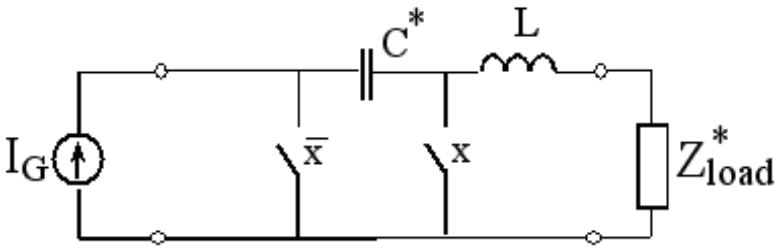

Figure 18: The resulting current buck-boost topology.

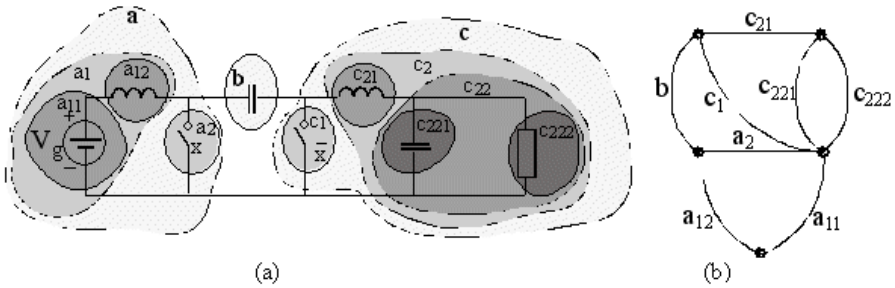

Figure 19: A voltage Čuk topology (a) and its graph description (b).

Following the duality rules, the boost-buck current-to-current converter topology of Fig. 20 is reached, which exhibits continuous input and output voltage and current (in CCM), in similarity to the original voltage-to-voltage converter.

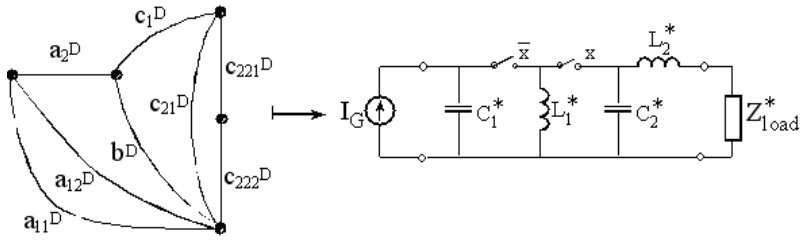

Figure 20: The resulting Čuk current topology.

The SEPIC voltage-to-voltage converter shown in Fig. 21 may be described by the same graph as the Čuk one (Fig. 19b) and the dual current-to-current converter topology described by the graph of Fig. 20. After components substitution, a current-to-current converter topology dual to the SEPIC is achieved, see Fig. 22.

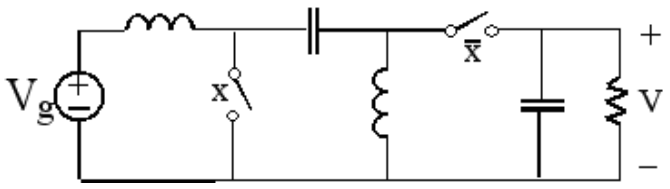

Figure 21: A voltage single ended primary inductance topology.

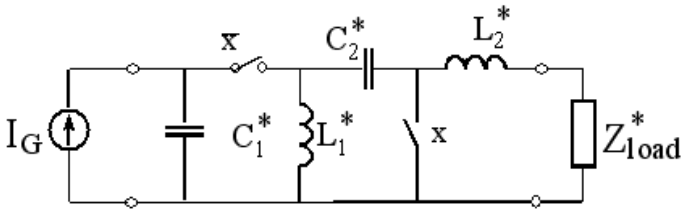

Figure 22: The resulting single ended primary inductance current topology.

4 A practical example

For a certain SMES project it was required to supply a DC, constant voltage load from a superconducting large coil, while controlling the rate of power flow and regulating the DC output voltage. It is motivated by the replacement of the storage batteries in an UPS system with a Superconducting Magnetic Energy Storage (SMES). Other applications include energizing of critical DC loads during voltage sags or outages.

4.1 Power stage

As the superconducting coil is a rather stiff current type of source, a current-to-current converter topology was required. The buck dual of Fig. 14 was chosen, with the switch implementation shown in Fig. 23.

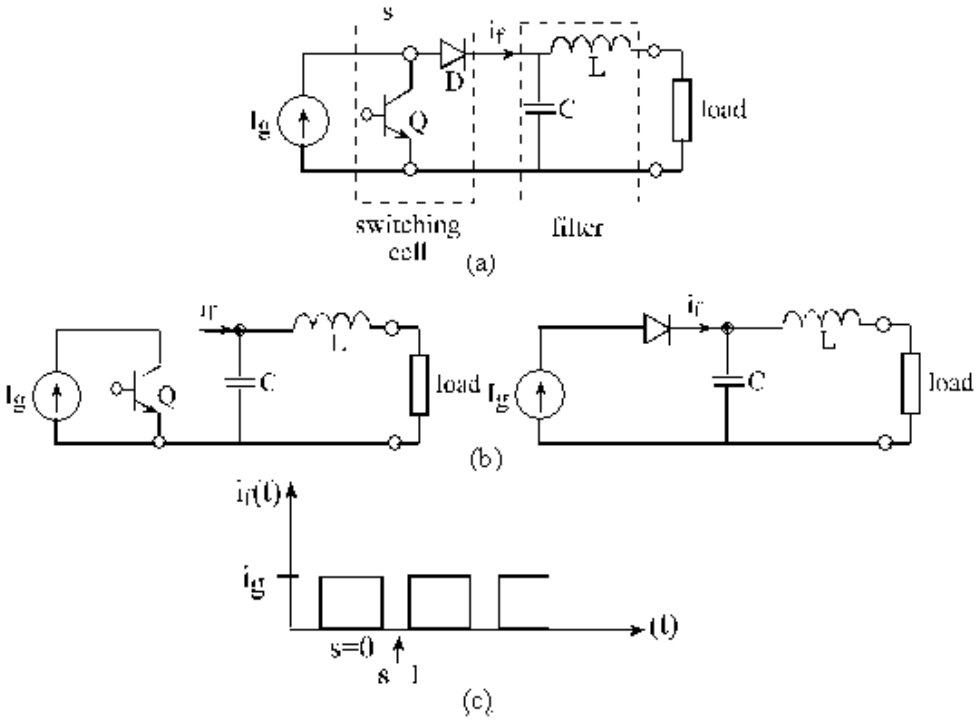

Figure 23: Power stage: (a) switch implementation; (b) two operation states; (c) filter input current.

The generator current is alternately diverted from the switch Q to the diode and vice versa. During the switch 'on' state, the switch provides a closed path for the source current and no energy is being supplied by the source. During the switch 'off' state, the source current is forced into the capacitor-inductor junction through the diode, delivering power from the source.

$$p_g(t) = \begin{cases} 0 & s = 1 \\ v_c(t) \cdot i_g(t) & s = 0 \end{cases}. \tag{9}$$

The average filter input current over a switching period is derived:

$$\langle i_f(t) \rangle_{T_S} = \langle (1 - d(t)) \cdot i_g(t) \rangle_{T_S}. \tag{10}$$

Since the input current hardly changes during a switching period and the duty ratio is actually defined as the on time during a switching period, equation (8) can be simplified:

$$\langle i_f(t) \rangle_{T_S} = (1 - d(t)) \cdot i_g(t). \tag{11}$$

With appropriate filter components, the ripple component of i_f flows through the capacitor while the DC component flows through the inductor and the load. The DC transfer function is derived:

$$V_o = (1 - D) \cdot I \cdot R_l. \tag{12}$$

Equation (12) shows that the load voltage is controllable via the duty ratio and thus the topology complies with the requirement no. 3. However, (12) also indicates that unlike as in conventional switched mode converters, the output voltage is inherently load dependent, thus output regulation is possible only with a closed loop mode. It can be seen from Fig. 23 that a pulsating current i_f is injected at the capacitor-inductor junction. As long as the capacitor presents an impedance, that is much lower than the inductor and load series combination, all of the current AC components may be assumed to flow through the capacitor while the current average flows through the inductor and load. Thus the capacitor current is a square wave with a peak-to-peak amplitude equal to that of the source i_g and zero DC component, see Fig. 24.

The resulting capacitor voltage ripple can be formulated as

$$\Delta v_c = \frac{d \cdot (1 - d) \cdot I_g}{2 \cdot f_S \cdot C}. \tag{13}$$

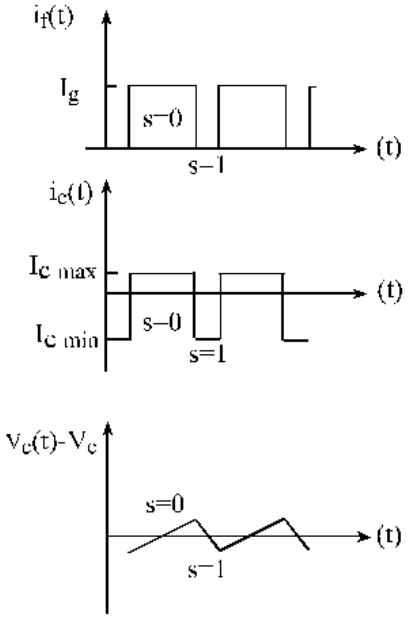

Figure 24: Main waveforms in the converter. Top to bottom: filter input current, capacitor current, and capacitor voltage ripple.

The maximum capacitor voltage ripple is:

$$\Delta v_c = \frac{I_g}{8 \cdot f_S \cdot C}. \tag{14}$$

Not all of this ripple develops on the load; there is an additional ripple reduction due to the inductor impedance. The maximum output ripple can be approximated as:

$$\Delta v_{load-\max} = \left. \frac{Z_{load}(\omega)}{Z_{load}(\omega) + j\omega L} \right|_{\omega_S} \cdot \frac{I_g}{8 \cdot f_S \cdot C}. \tag{15}$$

These expressions can serve for the selection of capacitor, inductor, and switching frequency according to the allowable ripple.

4.2 Power manipulation and SMES coil current decay profile

With given load, regulation of the output voltage means supplying a constant output power. Assuming low losses within the converter, this means a steady power throughput and a constant decrease of the energy stored in the

superconducting coil reservoir. The energy stored in the superconducting coil and the rate of discharge are

$$E_{SMES} = \frac{L_{SMES} \cdot i_g(t)^2}{2} \;\; ; \;\; \frac{d}{dt}(E_{SMES}) = p_{out} = \frac{V_{load}^2}{R_{load}} \;\; . \tag{16}$$

which yields the superconducting coil current:

$$i_g(t) = \sqrt{i_g(0)^2 - \frac{2 \cdot P \cdot t}{L_{SMES}}} = \sqrt{i_g(0)^2 - \frac{2 \cdot V_{load}^2 \cdot t}{L_{SMES} \cdot R_{load}}}. \tag{17}$$

The duty ratio variation over the discharge time is found by substituting (17) into (11).

$$d(t) = 1 - \frac{V_{load}}{\sqrt{i_g(0)^2 - \frac{2 \cdot P \cdot t}{L_{SMES}}} \cdot R_{load}} = 1 - \frac{V_{load}}{\sqrt{i_g(0)^2 \cdot R_{load}^2 - \frac{2 \cdot V_{load}^2 \cdot R_{load} \cdot t}{L_{SMES}}}} \tag{18}$$

which indicates that output regulation is lost at t_{cr}, shortly before all the stored energy is exhausted.

$$t_{cr} = \frac{1}{2}\left(\frac{i_g(0) \cdot L_{SMES} \cdot R_l}{V_l^2} - \frac{L_{SMES}}{R_l}\right). \tag{19}$$

These equations are in agreement with the SPISE simulation results shown in the next section.

4.3 Small signal analysis

Figure 25 shows a low-frequency model of the proposed converter in which the switching network was replaced by two dependent sources.

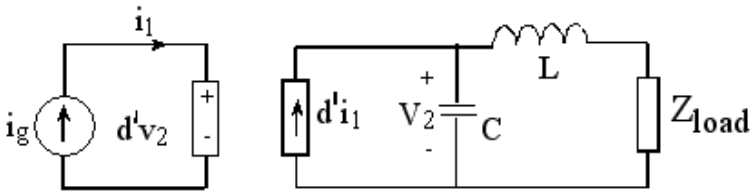

Figure 25: Low frequency AC model of the converter.

Accounting to frequencies much lower than the switching frequency [1], this model provides a fair approximation for both large and small signals.

For the small signal analysis an averaged switch network replaces the switch, which is equivalent to 'perturbation and linearization' process [1], see Fig. 26.

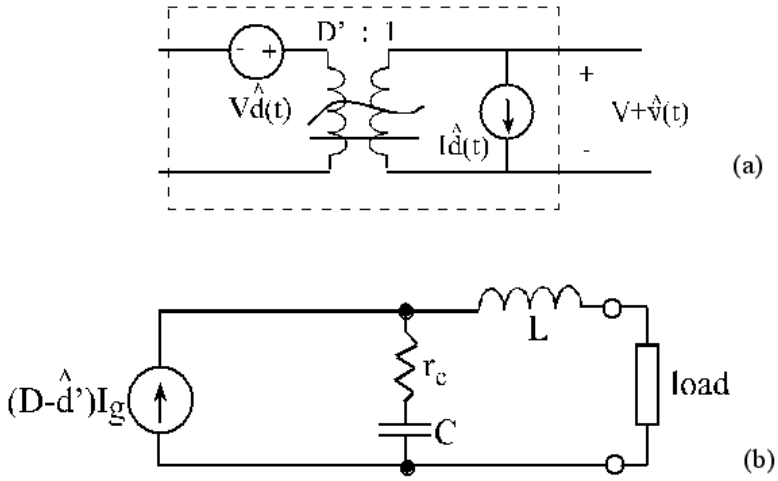

Figure 26: Averaged switch model (a) and the converter small signal model (b).

In addition, the model was augmented by the equivalent series resistance (ESR) of the capacitor, r_C. Modeling of the inductor resistance is not needed since it is included in the load resistance. After some circuit manipulation, a simplified model which models the small signal behavior is reached and shown in Fig. 26b. This model has a simple transfer function with two poles and one zero in the LHP.

$$\hat{v}_{load} = \frac{r_C \cdot R_{load} \cdot \left(D' - \hat{d}'\right)}{L} \cdot \frac{S + \frac{1}{r_C \cdot C}}{S^2 + \left(\frac{r_C + R_{load}}{L}\right) \cdot S + \frac{1}{L \cdot C}} \cdot i_g. \qquad (20)$$

As it can be observed, this topology is unconditionally stable for duty ratios in the range of $0 \div 1$.

4.4 Simulation and experimental results

The circuit is meant to connect to a UPS DC bus at its output, therefore the converter output is regulated at 400 Volt. The power stage linearized transfer function (19) was employed for the derivation of the controller.

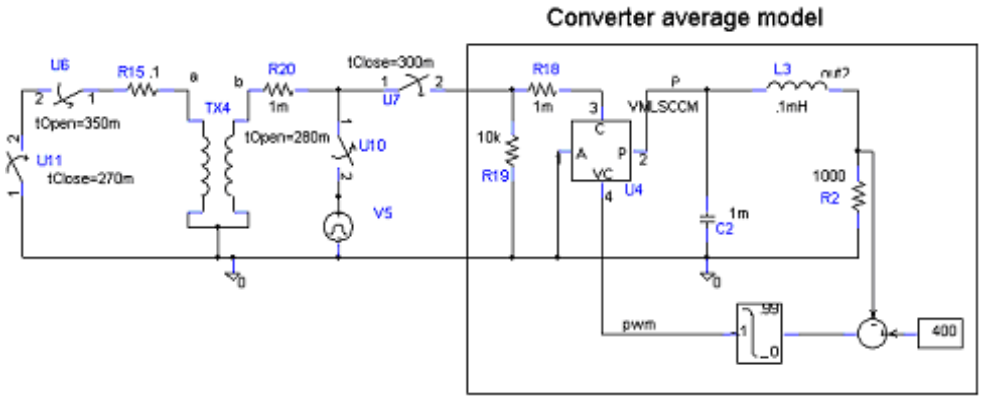

Figure 27: The average model simulation scheme.

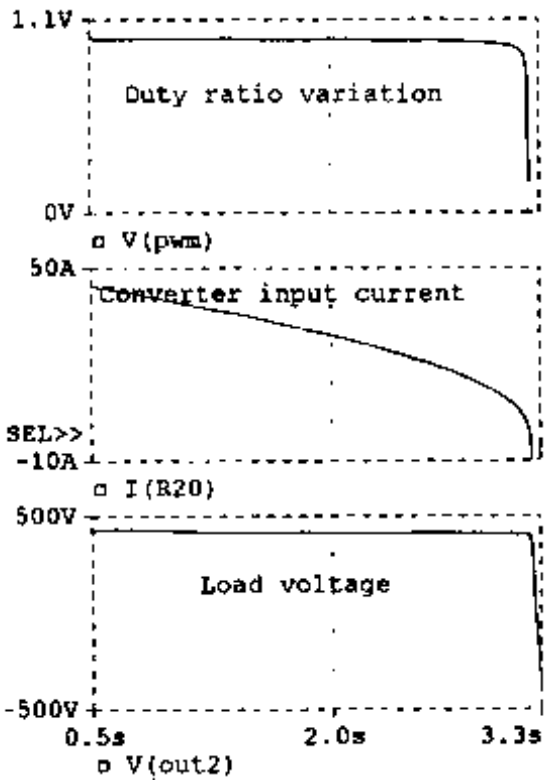

Figure 28: The average model simulation results.

The circuit was simulated by SPICE software, first with averaged models and later using switching models. The average model is shown in Fig. 27, the focus is on the converter section while the rest of the scheme is about charging and protecting the SMES coil.

The SMES coil is assumed to have an inductance of 0.5H and be initially charged to almost 50A. The average mode simulation results are shown in Fig. 28.

The satisfactory load voltage regulation can be noticed as well as the duty ratio and current variation, in accordance with (17) and (18). For the switching detailed simulation, a switching circuit with realistic component models replaced the average model of Fig. 28. A simple voltage mode modulator was incorporated. The output is well regulated until all the superconductor energy is exhausted (at $t \sim 86$ms). The parabolic profile of current decrease may be noticed, in accordance with (17) and (18) and with the average model simulation, see Fig. 29.

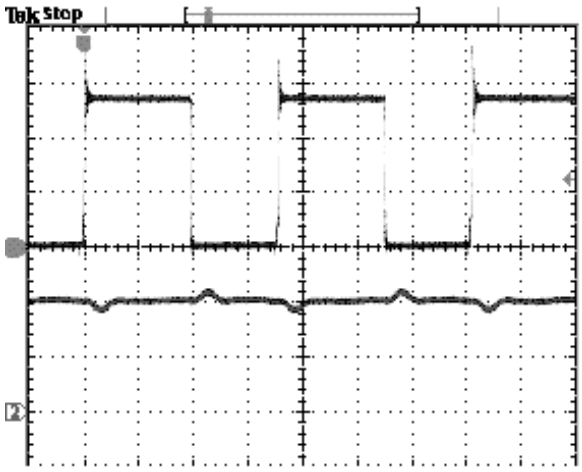

Figure 29: Converter input voltage (ch1 20V/div), and input current (ch2 2A/div).

Experimental results are presented for a partial loading of 110 Watt, down sized prototype. In the experimental setup a 470μF capacitor and 20μH inductor were used and the switching frequency was 70kHz. The input current I_G is 4A. The output is regulated at 50V and the load is a 22Ω resistor. Typical waveforms are presented in Fig. 30.

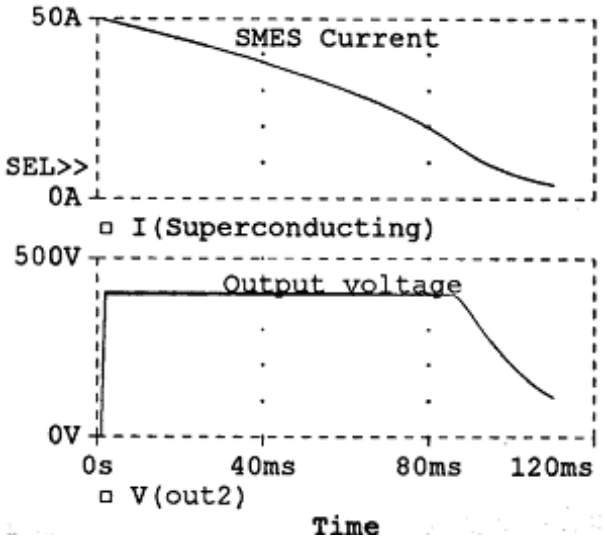

Figure 30: Simulation results in the switched mode.

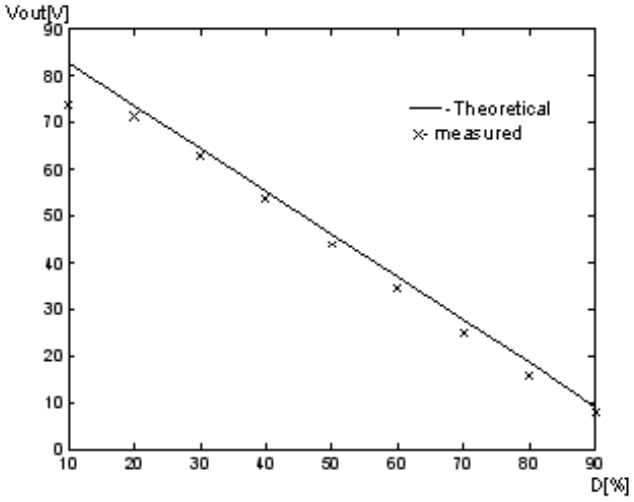

Figure 31: Experimental steady state transfer ratio of the dual buck at I_g= 4A.

The steady state transfer ratio from input current to output voltage is shown in Fig. 31, which agrees with (12). Due to simplicity and low component count, high efficiency is achieved even with hard switching, see Fig. 31.

A dual buck-boost current converter was build and tested at the same power level as well.

Comparison between theoretical and experimental results is provided in Fig. 32.

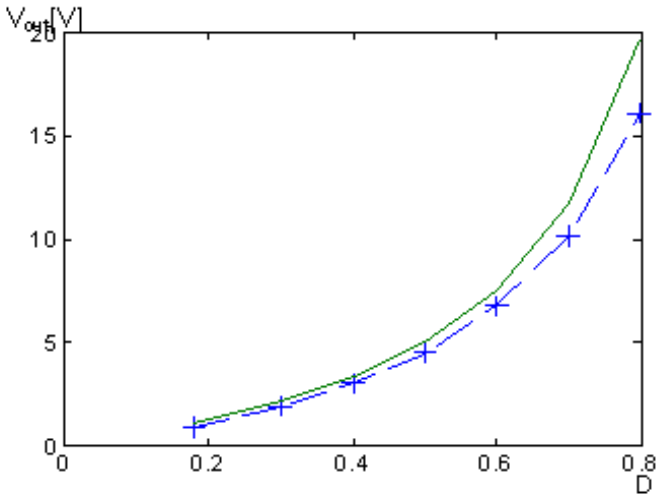

Figure 32: Experimental steady state transfer ratio of the dual buck-boost converter at I_g= 4A.

5 Conclusions

A unified approach for the derivation of current-to-current converter topologies was presented. In this method, previously known duality principles are augmented by the application of cascaded two port elements and functional analysis of circuits, as well as by the successive application of series/parallel transformation. Switching bridges are modeled by a virtual variable-transformer, which greatly simplifies the treatment of circuits containing transformers and switching bridges. Thus, a universal tool for

derivation of current-to-current converters by dually transforming voltage-to-voltage converter topologies was developed. Some examples for the application of this method show its consistency.

Experimental results for a practical design of a current-to-current converter for SMES (Superconducting Magnetic Energy Storage) application were also provided.

References

[1] R. Erickson, *Fundamentals of Power Electronics* (Chapman and Hall, N.Y., 1997).

[2] M. Ehsani and R.L. Kustom, *Converter Circuits for Superconductive Magnetic Energy Storage* (Texas A&M University Press, 1988).

[3] M. Ehsani, R.L. Kustom and R.E. Fuja, IEEE Trans. on Industry Applications **19**, 690 (1983).

[4] D. Shmilovitz and S. Singer, 17-th Annual Applied IEEE Power Electronics Conference and Exposition, APEC'2002, p.630 (2002).

[5] R. Rabinovici and V. Tentser, 8th Int. Conference on Optimization of Electric and Electronic Equipment (Optim'2002), Brasov, Romania, 16-17 May, 2002, p.269 (2002).

[6] M. Ehsani, J. Mahdavi, I. Pitel, J.E. Brandenberg, and F.E. Little, IEEE Aerospace & Electronic Systems Magazine **13**, 37 (1998).

[7] M. Milanovic, I. Godec, and F. Mihalic, 27-th Annual IEEE Power Electronics Specialists Conference (PESC'96), Baveno, Italy, 23-27 June 1996, vol.**2**, p.1294 (1996).

[8] M. Kazimierczuk, and D. Czarkowski, *Resonant Power Converters* (Wiley, N.Y., 1995).

[9] M. Ehsani, M.O. Bilgic, A.D. Patton, and J. Mitra, IEEE Aerospace & Electronic Systems Magazine **10**, 3 (1995).

[10] S. Singer, D. Shmilovitz, Y. Ifrah, and I. Cohen, IEEE Trans. on Power Electronics **10**, 239 (1995).

[11] H. Ohguchi, M.H. Ohsato, T. Shimizu, and G. Kimura, IEEE Trans. on Power Electronics **13**, 1023 (1998).

[12] L. Martinez-Salamero, J. Calvente, R. Giral, A. Poveda, and E. Fossas, IEEE Transactions on Circuits & Systems I **45**, 355 (1998).

[13] R. Rabinovici and B.Z. Kaplan, IEEE Electronics Letters **27**, 1948 (1991).

[14] P.J. Wolfs, K.C. Kwong, and G.F. Ledwich, IEEE Transactions on Power Electronics **7**, 683 (1992).

[15] P.J. Wolfs, IEEE Transactions on Industrial Electronics **40**, 139 (1993).

[16] P.J. Wolfs, G.F. Ledwich, and K.C. Kwong, IEEE Transactions on Power Electronics **8**, 104 (1993).

[17] C.A. Desoer and E.S. Kuh, *Basic Circuit Theory.* New York, p.444 (McGraw Hill, N.Y., 1969).

[18] N. Balabanian and T.A. Bickart, *Electrical Network Theory.* p.122 (Willey, N.Y., 1969).

[19] S. Čuk, IEEE Power Electronics Specialists (PESC'79), p.109 (1979).

[20] R.P. Severns and G.E. Bloom, *Modern DC to DC Switched Mode Power Converter Circuits* (Van Nostrad Reinhold, N.Y., 1985).

[21] S.D. Freeland, IEEE Power Electronics Specialists (PESC'89) p.114 (1989).

[22] S.D. Freeland, IEEE Transactions on Power Electronics **7**, 374 (1992).